Proceedings of 2014 IEEE
International Conference on Mechatronics and Automation
August 3 - 6, Tianjin, China

New Approach for Modeling and Testing of Harmonic Drive in Robotic Systems

Shimeng Li and Yuan F. Zheng*
Department of Electrical and Computer Engineering
The Ohio State University
Columbus, Ohio 43210, USA
{li.2212 & zheng.5}@osu.edu

Lei (Raymond) Cao
Department of Mechanical and Aerospace Engineering
The Ohio State University
Columbus, Ohio 43210, USA
Cao.152@ osu.edu

***Abstract* - Harmonic drives are becoming a key component in advanced robotic systems. The complicated dynamic behavior of the harmonic drive is due to the nonlinear torsional stiffness and hysteresis. Traditional modeling methods capture the behavior patterns of the harmonic drive by treating it as a black box in the experiments. This paper provides a new dynamic modeling method which takes into consideration component interactions inside the harmonic drive. In addition an innovative method for testing the performance of the drive is devised. Based on this new method, we have developed a testing station and performed experiments on a real harmonic drive which is used in the Hubo+ humanoid robot. The testing results have verified the new modeling and testing method.**

Index Terms* - *harmonic drive; dynamic modeling; Hubo+; robotic systems; testing method

I. INTRODUCTION

The harmonic drive gear was developed by C. Walton Musser in the 1957. Unlike traditional speed reduction systems, it can achieve high gear ratio with features of compact, light-weight, and small-size; so it is highly favored for electromechanical systems with space and weight constraints. Particularly, the advantages of the harmonic drive such as zero-backlash, low frictional losses, accuracy, and high torque capacity make itself ideal for robotic applications [1]. In recent years, harmonic drives have become even more popular due to the emerging of advanced robotic systems such as humanoid robots. The Hubo+ humanoid robot platform in Fig. 1(a) is an example of harmonic drive applications in one of the most advanced humanoid robotic systems at present. The Hubo+ humanoid robot platform has 41 degrees of freedom (DOF) in total (12 in each of the two legs, 8 in each of the two arms, 14 in hand, 6 in head, and 1 in trunk). On each DOF there is one harmonic drive used for speed reduction driven by brushless DC motor (Fig 1(b)). The Hubo+ humanoid robot can do smooth motions such as hand shaking and Taichi. It can also perform powerful actions such as keeping balance on one leg. With the control scheme implemented, Hubo+ can reach the speed of 1.8 km/hr for normal biped walking on flat surface [2, 3]. In addition, harmonic drives have been used in other high-end dynamic systems for motion control such as printing machines, and aircrafts and rockets in the aerospace industry. Due to the significant rise of applications, users as well as developers of harmonic drives become interested in simple and efficient modeling and testing methods of harmonic drives. The goal is to select adequate devices which can perform as the system designers intend while keeping the cost in check.

The outstanding performance of the harmonic drive depends on its ingenious design by taking advantage of the flexible material, which gives unique features to its transmission kinematics and dynamics. A harmonic drive consists of three main components: the wave generator, the flexspline, and the circular spline (Fig. 2 (a)) plus supporting components such as bearings and housings. Particularly different from the traditional gear spline, the flexspline is a thin-walled flexible cup adorned with small external teeth around its rim. The transmission principle between these three components is shown in Fig. 2 (b). When assembled, the wave generator is nested inside the flexspline, causing the flexible gear teeth circumference on the flexspline to adopt the elliptical profile of the wave generator; the external teeth on the flexspline mesh with the internal teeth on the circular spline along the major axis of the wave generator ellipse. The flexspline is always designed a fewer teeth than the circular spline. As the circular spline is fixed, every circle the wave generator rotates the teeth on flexspline mesh with the teeth on circular spline continuously, and left the few teeth offset in angular position on the opposite direction. So the ideal position relationship of the harmonic drive wave generator, flexspline and circular spline can be represented as:

$$\theta_{wg} = (N+1)\theta_{cs} - N\theta_{fs} \quad (1)$$

where θ_{wg} is the angular position of the wave generator, θ_{cs} and θ_{fs} are the angular position of circular spline and flexspline, respectively. In most cases, $\theta_{cs} = 0$. N is the normalized gear ratio of harmonic drive, so

$$N = \frac{N_{cs}}{N_{cs} - N_{fs}} \quad (2)$$

where N_{cs} is the number of teeth on the circular spline N_{fs} is the number of teeth on the flexspline. A harmonic drive can reach the gear ratio from 30:1 up to 320:1, which is not possible for traditional gear reduction system [5].

The degradation of harmonic drive performance is caused by the three main nonlinear dynamic features: nonlinear friction, torsional stiffness, and positional error. These nonlinear features cause disturbances such as kinematic error and hysteresis effect in harmonic drive transmission and make it difficult for accurate modeling of the behavior of harmonic drive [6].

In previous studies related to the modeling of harmonic drive nonlinear features, experimental observations of

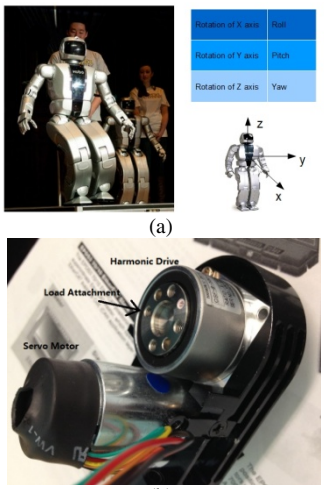

Fig. 1 Hubo+ humanoid robot platform (a) and the structure of robot wrist joint (b)

transmission are made to identify the typical response patterns, and nonlinear models are developed to capture the complexity of the observed responses. This "experiment and model" method is described in the work by Tuttle and Seering [7], which employs nonlinear modeling to describe the profile of the harmonic drive positional error, torsional stiffness, and friction. The same method is used in the modeling of harmonic drive hysteresis by Dhaouadi [6], modeling of kinematic error by Ghorbel [8], and modeling of nonlinearity in other approaches in [9- 11].

The harmonic drive testing system used in those approaches is generally based on the idea of the "McGill Testing Station" which was first developed at the Centre for Intelligent Machines in McGill University [12]. The harmonic drive is driven by a DC motor controlled by a servo amplifier. The station has two different setups to test the free motion and constrained motion, which are switched between by the positive lock. Position and torque sensors are used on both input and output ends of harmonic drive, by which the harmonic drive transmission system is treated as a "black box". By giving different motor patterns to the input of harmonic drive, one can obtain the corresponding motion profile at the output end and then analyze the performance. The limitation of the testing system is that the sensor reading from the output end is the fusion of hysteresis and kinematic error information resulted in by comprehensive nonlinear factors inside the harmonic drive [6][8]. That means that under this condition, it is difficult to obtain a sensor reading profile that can reveal the internal nonlinear dynamic features of harmonic drive, which degrades the modelling validity due to the introduction of uncertain factors.

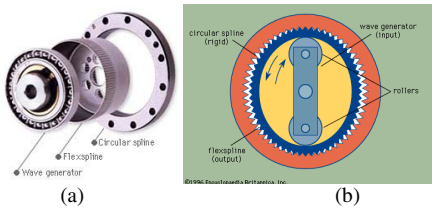

Fig. 2 Harmonic drive components (a) and transmission principle (b) [4]

Our approach provides a new method studying harmonic drive transmission modeling which overcomes the limitation of previous approaches. Based on analyzing the interaction between components inside the harmonic drive, we are able to establish the dynamic model of the harmonic drive transmission system analytically without just treating it as a "black box". Moreover, in order to study the detailed nonlinear features of component interactions, we have designed a new approach for testing the modeling of harmonic drive, setup the experiment and showed results to prove the theoretical validity.

This paper is organized as following: the second section introduces the nonlinear factors of the harmonic drive transmission; the third section analyzes the component interactions inside the harmonic drive and gives a dynamic modeling based on the analysis; the forth section explains our idea of the new testing method and shows our experimental setup; the fifth section is on the analysis of testing results and verify the theory of our approach. The paper is concluded by the sixth section.

II. Nonlinear Factors of Harmonic Drive Transmission

A. *Positional Error*

The concept of "positional error" is not actually what we defined as "output kinematic error" in the harmonic drive transmission. The output kinematic error can be defined as the difference between the motor input position and the harmonic drive output position considering the gear reduction ratio, as is shown in Fig. 3. A typical output kinematic error can be separated into two components: one is the pure positional error, and the other is the flexibility induced error [8].

The positional error is caused by the slight misalignment or deflection of shaft which will cause vibration, by which the flexspline teeth will move deeper in one side along the main axis of the wave generator periodically. A Fourier series expansion is used to express the periodic positional error as a function of the displacement θ_m [8]:

$$\tilde{\theta}_p = \frac{a_0}{2} + \sum_{n=1}^{k}[a_n \cos(n\theta_m) + b_n \sin(n\theta_m)] \qquad (3)$$

where a_0, a_n, and b_n are constant and Fourier coeffiecients. In assembled harmonic drives, there are always small intervals between the tooth meshing of flexspline and circular spline. While the input shaft is rotating with servo motor, there is small vibration on the output end of flexspline because the flexspline teeth always move deeper in one side along the main axis of the wave generator. So in (3), the pure positional error in harmonic drive transmission is a periodic signal with frequency equal to the rotation velocity of motor θ_m.

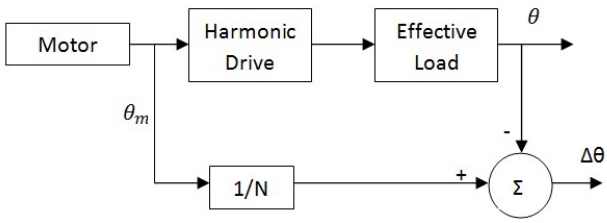

Fig. 3 Output kinematic error in harmonic drive transmission

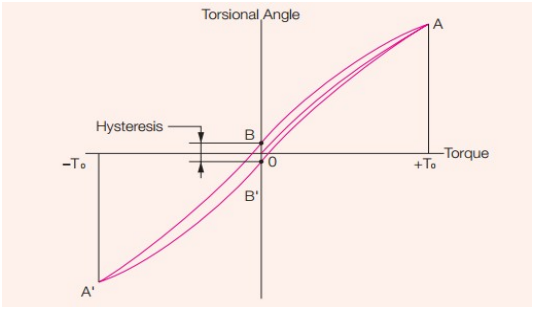

Fig. 4 Harmonic drive torsional stiffness profile [16]

B. *Torsional Stiffness*

Torsional stiffness (or compliance) is described as the relationship between torque and positional displacement in torsion with input rotationally locked. The torque-torsion curve is shown in Fig. 4 [16] as the applied torque goes back and forth within a certain range. In the curve we can see that the stiffness is increasing with torsional angle, and there is hysteresis effect in the torsional angle while the applied torque is zero. The physical explanation of the hysteresis effect can be found in [13] which results from the loop generated by the parallel elastic-slide motions inside the harmonic drive. The hysteresis effect takes place in normal transmission and causes positional kinematic error which is also called "flexibility induced error" in [8].

Despite the hysteresis effect in torsional stiffness, we can just use a cubic function to replicate the torsion-torque relationship [14, 15]:

$$\mathrm{T_k}(\Delta\theta) = \mathrm{k_1}(\Delta\theta) + \mathrm{k_2}(\Delta\theta)^3 \tag{4}$$

where $\mathrm{k_1}$ and $\mathrm{k_2}$ are coefficients, $\Delta\theta$ is the torsional displacement. In most cases $\mathrm{k_1}$ is much greater than $\mathrm{k_2}$ so usually we use a linear piecewise function to represent the torsion-torque relationship of the harmonic drive.

C. *Nonlinear Friction*

Frictions inside the harmonic drive exist on the contact of the lubricated surfaces between shaft, bearings, wave generator, flexspline and circular spline gear meshing. Friction between two lubricated surfaces is a function of relative angular velocity and can be characterized using a Stribeck friction model [17]:

$$\tau^{(f)}(\dot{\theta}) = sign(\dot{\theta})\left(\tau^{(f,C)} + \left(\tau^{(f,s)} - \tau^{(f,C)}\right)e^{-\left|\frac{\dot{\theta}}{\theta^{(s)}}\right|^{\delta}}\right) + c^{(v)}\dot{\theta} \tag{5}$$

where $\dot{\theta}$ is the angular velocity of joint, $\tau^{(f,C)}$, $\tau^{(f,s)}$ are friction torque parameters, and $c^{(v)}$is viscosity coefficient.

III. Component Interactions and System Modeling

Previous studies always use a methodology of a "black box" in modeling the harmonic drive. Researchers use kinematic error signal as shown in Fig. 3 to describe the nonlinear features in the harmonic drive transmission. This is because the compact design of the harmonic drive makes it impossible to put sensors in. Also, since the input of motor drive is the dominating factor in the normal operation of the harmonic drive, the studies have to focus on the small errors in the transmission to model the nonlinear factors. In fact, the key feature of the harmonic drive transmission is the interactions between components especially the torque and position transmission through the harmonic drive flexspline. We have developed an analytical method to give a more detailed view of the component interactions inside the harmonic drive and further build up a dynamic system modeling of the harmonic drive transmission. The details are described in the reminder of this section.

A. *Component Interactions inside the Harmonic Drive*

Fig. 5 shows the mechanical structure inside the harmonic drive. The circular spline is fixed on the housing and meshed with the flexspline tooth profile. The wave generator is connected with input shaft and mounted inside the flexspline cylinder by an elastic bearing on the input end of flexspline. The output shaft is connected with the output end of the flexspline and mounted through the housing by a bearing. To analyze the component interactions inside the harmonic drive, the most important and difficult part is to understand the torque and position transmission through the deformation of the harmonic drive flexspline.

Fig. 6 shows the geometric deformation of flexspline when the wave generator rotates inside harmonic drive. Since the input end of the flexspline cylinder is restricted by the eclipse shape of the wave generator, there will be a radial displacement w on the neutral curve; if the wave generator turns by θ_{wg} the circumferential displacement will be $\varphi_c = -\theta_{wg}/N$ by the transmission relationship in (1). For an external torque τ applied on the output shaft, we can assume that the flexspline is in a torque balanced condition, so the relative position of the wave generator, the input end of the flexspline and the tooth meshing area is stiff enough. Then there will be a torsional displacement φ_f on the output end of flexspline:

$$\varphi_f = {T_k}^{-1}(\tau) \tag{6}$$

where $\mathrm{T_k}^{-1}(\tau)$ is the nonlinear torque-torsion relationship as an inverse function of (4).

So the displacement of the harmonic drive position output can be derived as

$$\theta = \varphi_c + \varphi_\mathrm{f} = -\theta_{wg}/N + {T_k}^{-1}(\tau). \tag{7}$$

For the torque transmitted from the output end to the wave generator, we can consider a ballanced condition on the input and output end of the flexspline without any dissapation. For the gear transmission ratio N:

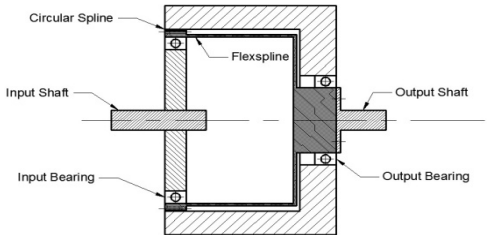

Fig. 5 Mechanical structure inside the harmonic drive

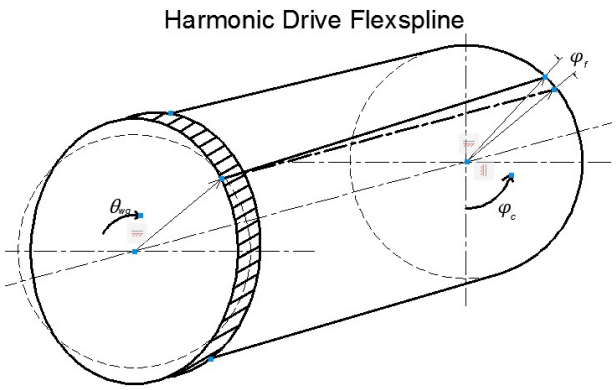

Fig. 6 Harmonic drive flexspline deformation

$$\tau_{wg} = -\tau_{fs}/N$$

where τ_{fs} is the torque applied to the output end of the flexspline. In normal cases τ_{wg} is a resistant torque that the wave generator has to overcome as well as the friction torque generated by the lubricated sliding motion between the shaft, the wave generator, the flexspline, and bearings on the input end.

B. *System Modeling Diagram*

Fig. 7 is our proposed harmonic drive dynamic transmission system modelling diagram. In Fig. 11, the input of the system is $\tau_d(t)$, which is the driving torque from the motor, and here we consider a simple DC motor that produces drive torque regardless of the sensors or feedback control scheme. The external load torque τ_l is treated as an environment parameter applied on the output end of the flexspline along with the output friction τ_{fout}. The linear factors in the system include the moment of inertia of the wave generator I_{wg} and the gear reduction ratio N; the nonlinear factors include the input damping torque $\tau_{din}(\dot{\theta}_{wg})$, the torsional displacement $\theta_f(\tau)$, and the positional error $\tilde{\theta}_p$.

The output position of the harmonic transmission system, as shown in Fig 7, can be represented as:

$$\theta_{out} = -\theta_{wg}/N + T_k^{-1}(\tau_l + \tau_{fout}) + \tilde{\theta}_p \quad (8)$$

For θ_{wg}, we can derive the dynamic transmission equation:

$$I_{wg}\ddot{\theta}_{wg} = \tau_d(t) - \frac{\tau_l + \tau_{fout}}{N} - \tau_{din}(\dot{\theta}_{wg}) \quad (9)$$

where $\tau_{din}(\dot{\theta}_{wg})$ indicates the viscous friction and damping on the input end of harmonic drive between the shaft, the wave generator, the flexspline and the bearings. These friction and damping factors are modeled as one because the lubricated friction depends on the viscosity which has a positive relationship with $\dot{\theta}$ in (5). For harmonic drives, the gear ratio can reach a very high value so in regular operation, the angular velocity of the wave generator $\dot{\theta}_{wg}$ is much higher than the angular velocity of the output end. That is why we can model τ_{fout} as a constant, also because its dynamic effect is divided by N while transmitted to the wave generator.

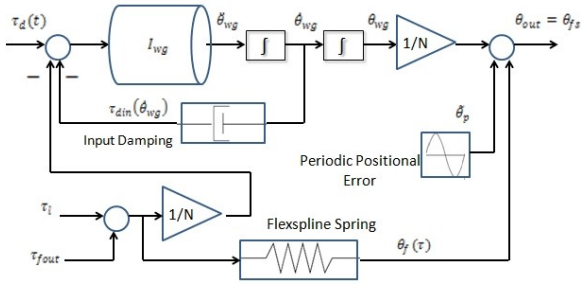

Fig. 7 Dynamic modeling diagram of the harmonic drive transmission system

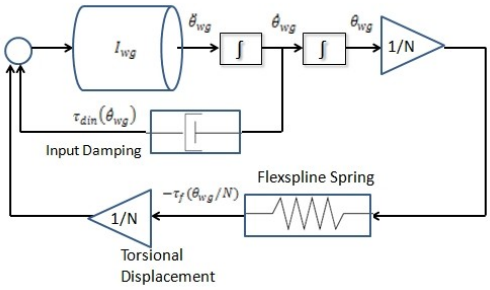

Fig. 8 Closed-loop dynamic diagram of the harmonic drive with no motor driving and output position locked

IV. Elastic-Slide-Free-Motion Testing Method for Harmonic Drive Nonlinear Features

A. *System Modification*

Previous harmonic drive modeling test methods rely on the sensor data of torque and position profile from both the input and output ends of the harmonic drive as we previously discussed. The reason is that different nonlinear factors in the harmonic drive transmission need to be modeled separately depending on their different dynamic features. However, it is still difficult to model the hysteresis effect, as it is a comprehensive effect resulted by the dynamic features of both frictional damping and torsional stiffness inside the harmonic drive [19]. Also in normal transmission, the kinematic error is dominated by the profile of the periodic positional error rather than the hysteresis induced error as is shown in Fig. 5 and Fig. 6, which makes it even more difficult to characterize the nonlinear factors simply by checking the difference between the input and output position signals.

To solve this problem, our approach is to establish a special condition for the harmonic drive modeling test to exclude some of the nonlinear factors and external dependencies. Consider a harmonic drive transmission system with 1) no motor drive input, and 2) output position locked. Then the entire system modeling diagram will be a closed-loop system as shown in Fig. 8.

In Fig. 8, since the output end of harmonic drive is locked, the vibration that causes the positional error is suppressed; so $\tilde{\theta}_p = 0$. If we give a displacement to the wave generator, the flexspline will be twisted and store elastic energy like a spring. With no external load or friction torque at the output end, the torsional torque will affect the behavior of the wave generator by a reduced factor of N. Then the entire dynamic equation of the system can be represented as below:

$$I_{wg}\ddot{\theta}_{wg} = -\tau_f(\theta_{wg}/N)/N - \tau_{din}(\dot{\theta}_{wg}) \quad (10)$$

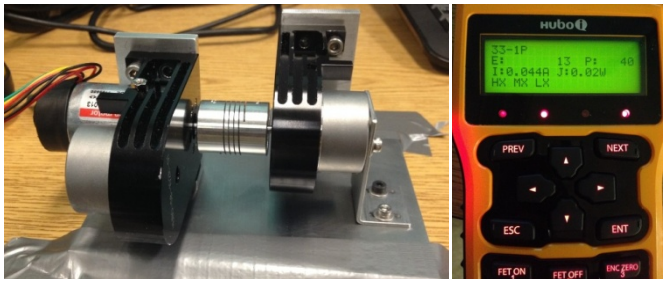

(a) (b)

Fig. 9 Harmonic drive "elastic-slide-free-motion" test station (a) and Hubo-I protocol commander (b)

where $-\tau_f(\theta_{wg}/N)$ is the torsional torque depending on θ_{wg}.

As is shown in (10), we now have a 2nd-order system to grasp the effects of the torsional stiffness and the damping inside the harmonic drive. We can use a cubic function in (4) to replicate the torsional torque τ_f, use a columb or Stribeck friction model in (5) to replicate the damping torque τ_{din}, and fix the parameters in the model by experiment data analysis and numerical simulation. However, as this approach has completely excluded the nonlinear positional error factor in the harmonic drive transmission, to gain advantages in modeling the torsional stiffness and the damping, traditional method is also needed to grasp the features of the nonlinear positional error if we need a complete model of the regular harmonic drive transmission.

B. Experimental Setup

Fig. 9 (a) shows the test station which is designed based on our approach. We use the CSF-8-100-2XH-F harmonic drive gearhead produced by the Harmonic Drive LLC [16] for testing. This type of harmonic drive is used in the wrist joint of Hubo+ humanoid robot platform. A Maxon brushless DC motor is linked to the harmonic drive input shaft by a coupler. All the components are mounted together and the output end of the harmonic drive is fixed at the bottom.

The function of the motor is to give an initial displacement to the wave generator and sense the angular position of the wave generator in real-time. Although this type of motor has very low damp, the moment of the rotor inertia should be added to that of the wave generator in the testing and modeling process. We used Hubo-I protocol commander [20] to control the motor (Fig. 9 (b)) and modified the source code from Rainbow GUI (Jungho Lee, jungho77@rainbow.re.kr) to read and store the position encoder value from the sensor inside the motor.

The updating frequency of the position encoder value has been set at 250Hz, and the resolution of the encoder value in Fig. 9 (b) is 0.00157 rad. By using Hubo-I, we can give an initial displacement value to the wave generator within a safe region without damaging the harmonic drive. This is achieved by setting up the over-current protection in the joint motor control board, and holding the position by turning on the servo and position control. The next step is to turn off the servo and enable the wave generator to rotate freely, following the closed-loop dynamics as shown in Fig. 8. We call this new method "elastic-slide-free-motion" test of the harmonic drive.

V. Testing Results

Fig. 10 shows the results of the experiments on our "elastic-slide-free-motion" test method. Parts (a), (b), and (c) are the results from using the same type of the harmonic drive CSF-8-100-2XH-F in order to test consistently the validity and repeatability of our method. The initial displacement has been set to ±0.157 rad and the free motion is started at zero second. The responses of the harmonic drive are then recorded by the sensor readings originally installed on the wrist joint of the Hubo+ Humanoid robot. The figures are plotted by MATLAB.

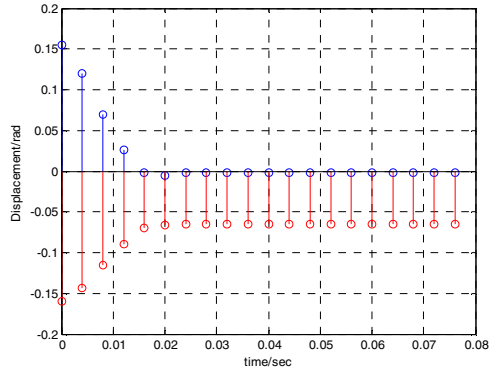

(a)

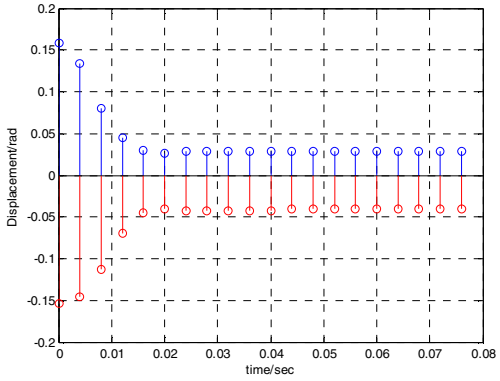

(b)

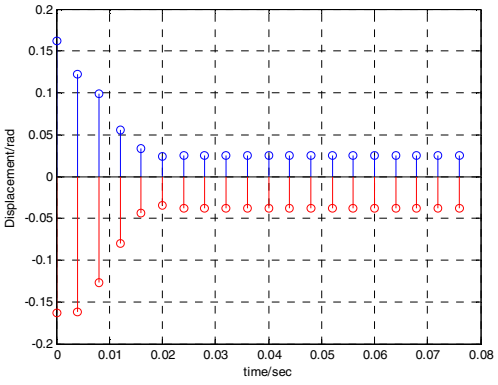

(c)

Fig. 10 "Elastic-slide-free-motion" test result of CSF-8-100-2XH-F harmonic drive

From the results, we can see that the free motion of the wave generator follows the response of a 2nd-order dynamic

system, and reaches the steady state in a short time at 0.02 second which also reveals a stable time constant related to the damping of the system. However, the steady state value of the wave generator position is not always zero. In fact, this is resulted from the natural backlash of the harmonic drive each time the testing station is adjusted or re-setup. The backlash region of the harmonic drive is naturally constant as we can see from the experiment that the region between the steady states of red (starting from -0.157 rad) and blue (starting from 0.157 rad) in (a), (b), and (c) are about 0.07 rad. The backlash of the harmonic drive also causes the soft wind-up effect in the harmonic drive testing by which the stiffness is decreasing rapidly when it is in low torsion [10].

In the backlash region, the torsional torque is not able to overcome the static friction inside the harmonic drive, which results in large error in the sensor reading [10]. This effect is also the cause of the hysteresis effect in the testing of the harmonic drive torsional stiffness in [13], and the small amount of backlash in the general operation of the harmonic drive. With the backlash region of the harmonic drive measured along with the 2nd-order nonlinear elastic-slide-free-motion dynamics, we should be able to establish a more precise model for the nonlinear characteristics in the harmonic drive.

VI. Conclusion

The harmonic drive has been a device used in robotic system for a long time. In recent years, the devices have become even more popular as the advent of more advanced robotics systems such as humanoid robots. The devices have also been actively used in high-end dynamic systems for motion control including printing machines, and aircrafts and rockets in the aerospace industry. More and more users as well as developers of harmonic drives become interested in simple and efficient modeling and testing methods of harmonic drives. In this paper, we have proposed such a modeling and testing method for harmonic drive. The method builds a dynamic system modeling, which gives a detailed view of inside component interactions, rather than treating the device as a black box by the previous method. Based on that, we have designed a new "elastic-slide-free-motion" harmonic drive testing method, developed the experiment test station, and analyzed the theoretical validity based on the experimental results. A complete model of harmonic drive transmission with the load added, such as a robotic joint, will be studied in our future research work.

Acknowledgment

This work was supported by the Defense Threat Reduction Agency of the United States Government under Contract HDTRA1-13-1-0012. The authors are solely responsible for the contents of this paper.

References

[1] H. Schempf and D. Yoerger, "Study of dominant performance characteristics in robot transmissions," *Journal of Mechanical Design*, Vol. 115, pp. 472-482, 1993

[2] Ill-Woo Park, Jung-Yup Kim, Jungho Lee, and Jun-Ho Oh, "Online free walking trajectory generation for biped humanoid robot (KHR-3 (HUBO)," in *Proc. the IEEE Int. Conf. on Robotics and Automation*, pp. 1231-1236, 2006.

[3] Hubo Humanoid Robot, http://www.ros.org/wiki/Robots/HUBO.

[4] T. D. Tuttle, "Understanding and modeling the behavior of a harmonic drive gear transmission," *AI Technical Reports*, May 1992.

[5] Harmonic Drive White Paper, http://www.electromate.com/db_support/attachments/Harmonic%20Drive%20White%20Paper.pdf.

[6] R. Dhaouadi and F. Ghorbel, "Modeling and analysis of hysteresis in harmonic drive gears," *Systems Analysis Model Simul*., Vol. 200, pp. 1-14, 2002.

[7] T. D. Tuttle and W. P. Seering, "A nonlinear model of a harmonic drive gear transmission," *IEEE Transactions on Robotics and Automation*, pp. 368-374, 1996.

[8] F. H. Ghorbel, P .S. Gandhi and F. Alpeter, "On the kinematic error in harmonic drive gears," *Transactions of the ASME*, Vol. 123, pp. 90-97, March 2001.

[9] C. W. Kennedy and J. P. Desai, "Estimation and modeling of the harmonic drive transmission in the Mitsubishi PA-10 robot arm," *IEEE Transactions on Intelligent Robots and Systems*, Vol.3, pp. 3331-3336, 2003.

[10] N. Kircanski, A. Goldenberg, and S. Jia, "An experimental study of nonlinear stiffness, hysteresis, and friction effects in robot joints with harmonic drives and torque sensors," in *Proc.* International Symposium *Experimental Robotics III*, Kyoto, Japan, pp. 326-340, 1994.

[11] T. Tjahjowidodo, F. Al-Bender and H. Van Brussel, "Nonlinear modelling and identification of torsional behaviour in harmonic drives," in *Proc. of ISMA*, pp. 2785-2795, 2006.

[12] Hamid D. Taghirad, "Robust torque control of harmonic drive systems," *IEEE Transactions on Robotics and Automation*, Vol.1, pp. 248 - 253, April 1997.

[13] Curt Preissner et. al., "A high-fidelity harmonic drive model," *ASME Journal of Dynamic Systems, Measurements, and Control*, Vol. 134(1), pp.0110002-1 -0110002-13, 2011

[14] T. Hidaka et al. "Vibration of a strain-wave gearing," in *Proc. International Power Transmission and Gearing Conference—New Technology Power Transmission*, pp. 789-794, 1990.

[15] D. P. Volkov, Y. N. Zubkov, "Vibrations in drive with a harmonic gear transmission," *Russian Eng. J.,* Vol. 58, No. 5, pp. 11-15, 1978.

[16] Harmonic Drive CSF Miniature Gearheads, http://www.harmonicdrive.net/media/support/catalogs/pdf/csf-mini-5-14.pdf, *Harmonic Drive LLC*, August 2012.

[17] J.B. Jonker, R. R. Waiboer, and R. G. K. M. Aarts, "Modelling of joint friction in robotic manipulators with gear transmissions," *Computational Methods in Applied Sciences*, Vol. 4, pp. 221-243, 2007.

[18] Huimin Dong et al., "Elastic deformation characteristic of the flexspline in harmonic drive," *ASME/IFToMM International Conference on Reconfigurable Mechanisms and Robots*, pp. 363-369, June 2009.

[19] H.D. Taghirad, P.R. Bélanger, "Modelling and parameter identification of harmonic drive systems," *ASME Journal of Dynamic Systems, Measurements, and Control*, Vol. 120(4), pp. 439-444, 1997.

[20] Hubo-i Manual, http://dasl.mem.drexel.edu/~ducNguyen/hubo/hubo-i-manual/.